

Stick-Slip Friction and Energy Dissipation in Boundary Lubrication

Yajie Lei and Yongsheng Leng*

Department of Mechanical and Aerospace Engineering, The George Washington University, Washington, D.C. 20052, USA
(Received 20 April 2011; published 30 September 2011)

Shearing of a simple nonpolar film, right after the liquid-to-solid phase transition under nanometer confinement, is studied by using a liquid-vapor molecular dynamics simulation method. We find that, in contrast with the shear melting and recrystallization behavior of the solidlike phase during the stick-slip motion, interlayer slips within the film and wall slips at the wall-film interface are often observed. The ordered solidified film is well maintained during the slip. Through the time variations of the frictional force and potential energy change within the film, we find that both the friction dissipation during the slip and the potential energy decay after the slip in the solidified film take a fairly large portion of the total energy dissipation.

DOI: 10.1103/PhysRevLett.107.147801

PACS numbers: 62.10.+s, 62.20.Qp, 68.08.-p, 68.18.Jk

Stick-slip motion of solids over each other in boundary lubrication is a complicated phenomenon [1,2] and is often observed in our daily lives. This phenomenon has been studied through well-controlled surface force experiments [3–8] in the past decades. A common idea is, for simple nonpolar fluids [4], stick-slip friction is associated with the crystallization and shear melting of the confined film with a few molecular diameters thickness [9–11]. During the stick, a finite shear stress or static friction force is built up within the solidified film. When the maximum shear stress within the film is exceeded, shear melting of the film occurs, resulting in the slip motion of solids. This slip process proceeds until the recrystallization of the film begins. A phenomenological analysis showed that most of the friction dissipation occurred by the viscous heating of the shear-melted film during this slip [12]. What is lacking so far is that one cannot directly observe shear melting in surface force measurements. Recent simulation studies showed that in some cases shear within the film or at the film-wall interface is one possible scenario of the stick-slip friction [13,14]. Here we use liquid-vapor molecular dynamics simulations [15,16] to show that shear melting is not necessarily a pathway for the energy dissipation during the slip. Instead, boundary slips at the wall-fluid interfaces and interlayer slips within the film are the ways of energy dissipation. We find that, during the slip, the crystalline structure of the solidified film can be well maintained. Shear melting, if it occurs, would involve a large energy penalty to disrupt the crystalline structure of the solidified film.

In the liquid-vapor molecular dynamics simulation, a simple driving spring model is used to simulate normal compression and sliding friction. A liquid film of argon containing 4319 argon molecules is confined between two solid walls [see Fig. 1(a)]. Simulation box lengths along the lateral x and y directions are 76.59 and 3.71 nm, respectively. Periodic boundary conditions are applied in the lateral directions. The film geometry is invariant in the y

direction. Two side vapor phases surround the central liquid film. Under compression, the liquid film can be freely squeezed out along the x direction, making the lateral pressure negligibly low (comparable to the ambient condition) due to the existence of the vapor phase [16]. In such a way, scaling particle coordinates to control the lateral pressure becomes unnecessary [15]. With this new simulation method, our recent simulation studies [16] reproduced many features of the highly asymmetric force oscillation profiles in surface force experiments [4,5,17,18]. The Lennard-Jones atomic potential ($\epsilon = 0.24$ kcal/mol and $\sigma = 0.34$ nm) [19] is used for the argon-argon interaction. Each confining wall is composed of a central wall and two sidewalls. The main interest here is the interaction between the central wall and the argon film. We assume that they have the same interaction strength as the argon-argon interaction, i.e., $\epsilon_{\text{wall-fluid}} = \epsilon$. Recent quantum mechanical density functional theory calculations [20] showed that the interactions between methyl (Me) groups in octamethylcyclotetrasiloxane (OMCTS) molecules (a model lubricant widely used in surface force experiments) and those between Me and mica surface oxygen atoms have the same order of interaction strength as argon-argon and argon-wall interactions (i.e., $\epsilon_{\text{Me-mica}} = 0.27$ kcal/mol and $\sigma_{\text{Me-mica}} = 0.34$ nm, $\epsilon_{\text{Me-Me}} = 0.39$ kcal/mol and $\sigma_{\text{Me-Me}} = 0.35$ nm, respectively). Considering the bulky structure of OMCTS, the two cases should have approximately the same wetting behavior. The interaction between the two sidewalls and argon is reduced to $\frac{1}{4}\epsilon$ to keep argon molecules in this region in a liquid phase. The face-centered cubic (fcc) wall is assumed to have the same atomic radius as the argon molecules (i.e., $\sigma_{\text{wall-fluid}} = \sigma$). This may not be true in the realistic context. However, the deformation of the mica-glass substrate in surface force experiments will make interfacial atoms and molecules rearrange to create local energy minimum [21], equivalent to a commensurate contact. Therefore, the friction behavior studied in the present commensurate contact model should be general.

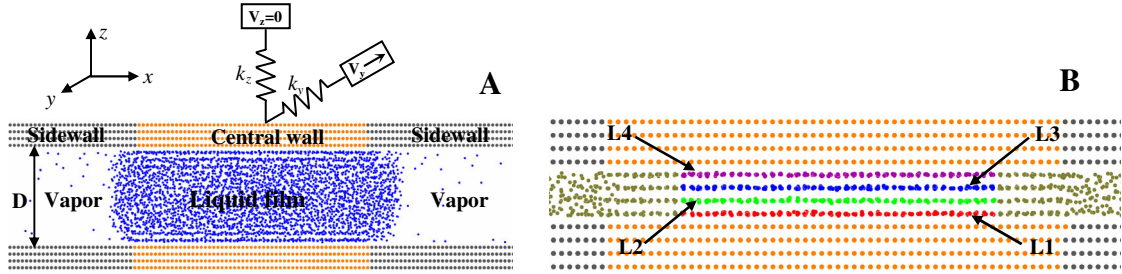


FIG. 1 (color online). (a) Schematic of the liquid-vapor molecular dynamics simulation geometry. (b) Snapshot of the equilibrium state of a four-monolayer solidified argon film confined between two solid walls. The argon monolayers in the solidified phase are represented by $L1$ – $L4$ with different colors. The central and sidewall atoms are represented by light red and gray dots, respectively.

Indeed, our recent studies showed that, when the wall and fluid molecules have different atomic radii, similar force oscillation and phase transition behaviors were also observed [16].

In this Letter, we focus on the stick-slip friction and energy dissipation mechanism of a simple argon film confined between two fcc crystal walls. Following the liquid-to-solid phase transition of an argon film at the $n = 7$ layer [16], we continue to compress the normal spring to squeeze the film to $n = 4$ ($D = 1.52$ nm), which is a more compact solidified film [see Fig. 1(b)] [16]. This is the typical number of monolayers for the study of stick-slip energy dissipation in the surface force experiment [12]. The sliding friction simulation is performed by pulling the top wall with the lateral spring along the negative y direction while holding the normal spring stationary at the compressive state [Fig. 1(a)]. We find that the normal spring force L fluctuates around 7.45 nN during sliding. The Nosé-Hoover thermostat is used to control the temperature of the argon film at 85 K. Since the sliding velocity of the upper wall is very small (see below), the dynamic behavior of the system will not be affected by the thermostat [22]. In simulations, only the forces acting on the discrete atoms of the top central wall are counted towards the total normal and lateral forces. This can effectively reduce the meniscus effect when the argon film is squeezed out substantially. The normal and lateral spring constants (k_z and k_y) are taken as 150 and 15 N/m, respectively. A softer lateral spring ($k_y = 15$ N/m) used in the sliding direction will provide a higher force resolution [16].

Figure 2(a) shows the stick-slip friction force versus the pulling distance of the spring at a driving velocity $v = 0.01$ m/s. Experiments and simulations [7,23] showed that the stick-slip behavior occurs when the sliding velocity is below a critical value v_c . This critical velocity is given by [23] $v_c = c(\sigma F_s/M)^{1/2}$, where c is a numerical factor between 0.05–0.5, F_s the maximum static friction force, and M the mass of the moving wall. Taking the values of $\sigma \sim 0.34$ nm, $F_s \sim 3$ nN, and $M \sim 5.3 \times 10^{-22}$ kg, we estimate that v_c is between 0.25 and 2.5 m/s. The current driving velocity is much smaller than the critical velocity v_c .

As the tension in the spring increases, the static friction force rises. When the maximum static friction force (the yield point) of the film is exceeded, we observe the shear behavior of the confined film which is dramatically different from the earlier studies [9,10]. We find that, instead of the shear melting of the film, the solidified film is well maintained during the slip, which undergoes boundary slips at the wall-film interface and interlayer slips within the film. These can be clearly seen in Figs. 2(b) and 3 from

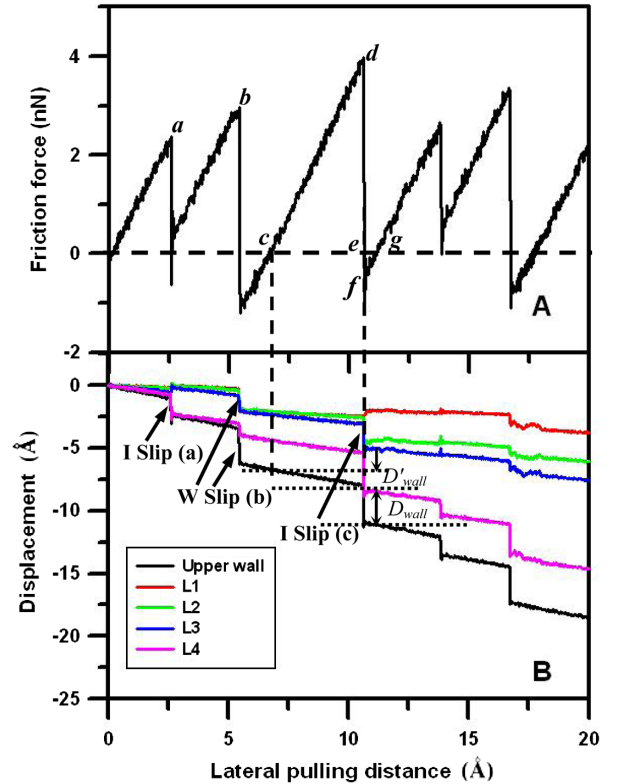


FIG. 2 (color online). (a) Variation of the stick-slip friction force as a function of the lateral pulling distance. (b) Displacement jumps of the top wall and the four monolayers in the solidified film. I slip and W slip refer to the interlayer and wall slips, respectively. D'_{wall} and D_{wall} are the wall displacements during the stick and slip in the c – f friction period, respectively.

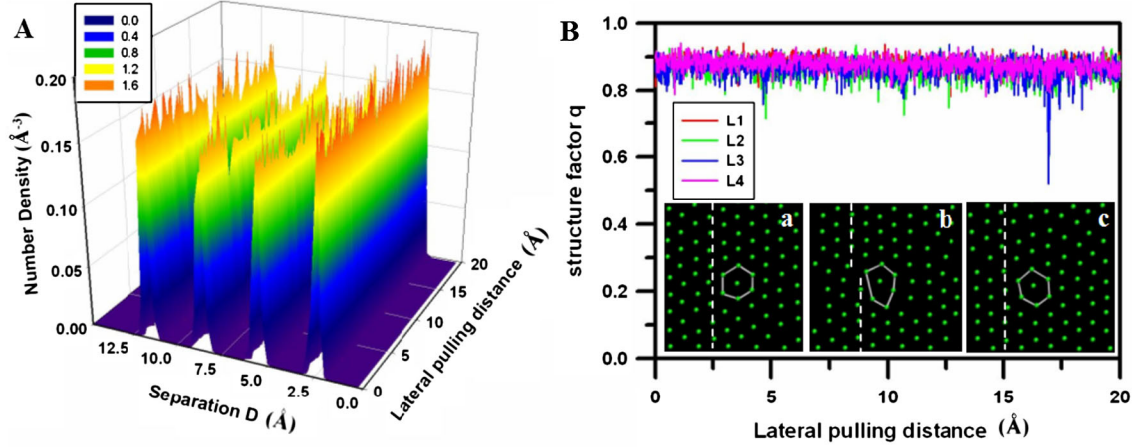


FIG. 3 (color online). (a) The number density distribution of argon molecules in the solidified film. (b) The variations of the in-plane structure factors q of $L1$ – $L4$ monolayers during the stick-slip motion. The broken dashed line in the inset panel b shows the lattice mismatch due to the distorted hcp structure of argon molecules during slip.

three aspects. First, Fig. 3(a) clearly shows the four distinct peaks of the argon density along the film thickness as a function of driving distance. These four peaks are well maintained during the stick-slip sliding, indicating a solid phase of the structure. Second, the in-plane structure factor q [19] [based on the hexagonal close-packed (hcp) crystalline structure [16]] of each monolayer, shown in Fig. 3(b), fluctuates around 0.9, further demonstrating the solidlike structure of the film. The slight drop in q to 0.5–0.7 during the slip does not originate from the shear melting of the confined film [10]; rather, it is due to the distorted hcp structure at the instant of slip [see the inset panel b in Fig. 3(b)]. The three snapshots in Fig. 3(b) show a typical series of molecular configurations for the $L2$ monolayer before, during, and after the slip. Finally, the boundary slips and interlayer slips within the film can be conceived by looking at the displacement jumps of different monolayers in Fig. 2(b). When the first yield point a in Fig. 2(a) is exceeded, Fig. 2(b) shows that the upper wall and $L4$ monolayer have the same amount of displacement jump, while the $L1$ – $L3$ monolayers stick with the bottom wall. This indicates that the interlayer slip occurs between the $L3$ and $L4$ monolayers within the film. The boundary slip occurs in the next displacement jumps in Fig. 2(b), corresponding to the yielding at point b in Fig. 2(a). Here we see the upper wall slip, signified by the different displacement jumps between the upper wall and the $L4$ monolayer, and the bottom wall slip, signified by the same amount of displacement jump for the $L1$ – $L4$ monolayers relative to the bottom wall. Both interlayer slips and wall slips are seen in the subsequent stick-slip motions. These slips result in sharp drops in spring forces [see Fig. 2(a)], from which a new stick-slip cycle begins. We find that the slip usually completes within ~ 20 ps, with a slip jump around 1–3 Å.

We now consider the energy dissipation during a typical stick-slip motion of the top wall [c – g in Fig. 2(a)].

Accompanying the increasing of the static friction force, the slow ramp-up of the displacement during the stick [Fig. 2(b)] corresponds to a gradual increasing of the potential energy in the solidified film. The total external work W_{ext} done by the driving spring (Fig. 1) to the molecular system is equal to the enclosed area c – e in Fig. 2(a), giving a value of $7.78 \text{ nN} \cdot \text{Å}$ ($1 \text{ nN} \cdot \text{Å} = 10^{-19} \text{ J}$). Prior to the slip, this energy is stored in the form of the elastic energy ΔE_{spr} in the spring and the potential energy ΔE_p in the solidified film. We find $\Delta E_{\text{spr}} = K_y \Delta x_0^2 / 2 = 5.07 \text{ nN} \cdot \text{Å}$, where x_0' is the extension of the spring during the stick, and $\Delta E_p = 2.24$ – $2.6 \text{ nN} \cdot \text{Å}$. The latter can be calculated either by the integration of the static friction force over the wall displacement [D'_{wall} in Fig. 2(b)] during the stick [24] or by the direct MD calculation of the potential energy increase of the solidified film. This potential energy stored in the solidified film takes about 30% of the total energy.

The key question is how the two energy components discussed above are dissipated during the slip. Figure 4(a) shows the variations of the friction force and the wall displacement versus time in a single slip event [d – f in Fig. 2(a)]. The two curves show that energy dissipation proceeds in two stages: the friction dissipation during the slip and the residual momentum loss of the top wall in the remaining ringing vibrations. These two processes are remarkably similar to those in the surface force measurement and phenomenological analyses [12]. In order to give a quantitative analysis, we consider the slip dynamics of the top wall. Figure 4(b) shows the very detailed slip behavior of the top wall in a much smaller time scale. The friction force (the spring force directly measured in the surface force experiments) F_y and the surface force W_y exerted on the top wall are shown in the inset in Fig. 4(b). These two forces are opposite in the stick and slip but become coherent in the subsequent ringing vibrations when the wall sticks with the film. Assuming that x_0 is

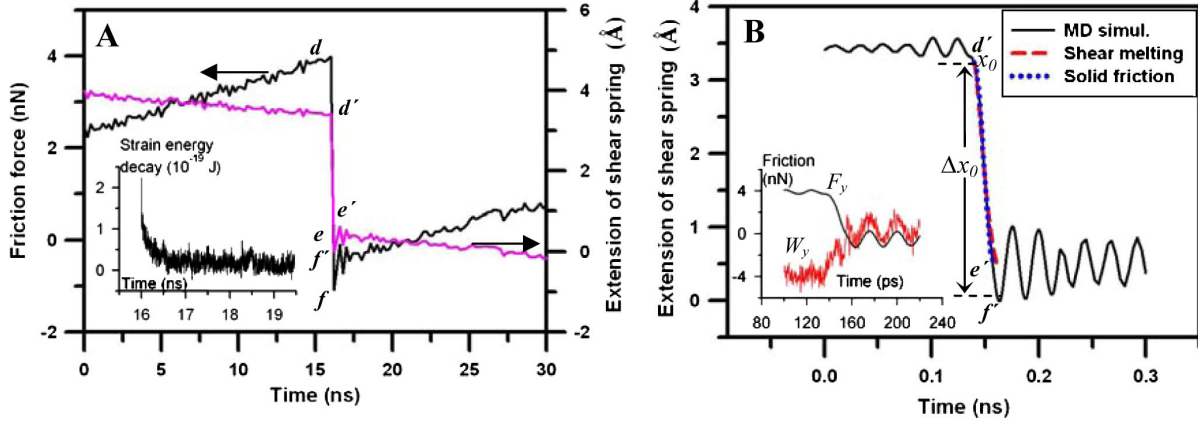


FIG. 4 (color online). (a) Friction force and displacement of top wall in a typical stick-slip cycle under a normal load of 7.45 nN. The inset shows the decay of the potential energy stored in the solidified film right after the slip. (b) Slip of the top wall at a smaller time scale. The blue dotted line corresponds to the $x(t)$ given by the solid friction model, and the red dashed line corresponds to the shear-melting model [12]. The inset shows the exact variations of the friction force F_y and surface force W_y during the short stick-slip-ringing period. Points d' , e' , and f' correspond to the maximum extension, zero extension, and maximum compression of the spring, respectively.

the maximum extension of the spring prior to the slip and $x(t)$ the instant position of the top wall during the slip, we can write the friction force as $F_y = k_y(x_0 + vt - x)$. Since the slip time of the top wall is only about 20 ps, the driving distance vt during the slip is much smaller than x_0 and can be omitted. The dynamic equation of the top wall can be written as $M(d^2x/dt^2) = k_y(x_0 - x) + W_y$. Here, M is the mass of the top wall, and k_y is the spring force constant. The surface force W_y in Fig. 4(b) is quite noisy, and it would be difficult to express this force in any simple function of time. However, if we assume that Amontons' law of solid friction [1] could be borrowed, i.e., $W_y = -\mu L$, where μ is the friction coefficient between argon monolayers or between the wall and film and L the normal load ($= 7.45$ nN), then we can solve the dynamic equation by using the initial conditions $x = (dx/dt) = 0$ at $t = 0$. Fitting the solution $x(t) = \alpha(1 - \cos\omega t)$, where $\alpha = (x_0 - \mu L/k_y)$ and $\omega = (k_y/M)^{1/2}$, to the actual slip curve $d' \rightarrow e'$ [Fig. 4(b)], we obtain a friction coefficient $\mu = 0.38$, a typical value for solid friction. Interestingly, if the shear-melting model is adopted [10,12], fitting the slip curve would give a very high effective shear viscosity for the confined film: $\eta_{\text{eff}} = 0.72$ Pa \cdot s [25]. This value is approximately 3 orders of magnitude larger than the bulk viscosity of liquid argon ($\eta_{\text{eff}} = 0.27 \times 10^{-3}$ Pa \cdot s at 85 K [26]).

It is known [12,24] that the dynamic equation discussed above fails to include the potential energy contribution ΔE_p stored in the confined film prior to slip. We point out that this is largely due to the inherent limitation of the phenomenological model. To illustrate this more clearly, we further examined the energy dissipation during the slip by integrating the dynamic equation of motion of the top wall over the slip distance $d' \rightarrow e'$ [Fig. 4(b)]. Point e'

corresponds to the zero spring force applied on the top wall where its slip velocity reaches 14 m/s. Integration of the dynamic equation with sliding distance yields [12] $\Delta E_{\text{kin}} = \Delta W_{\text{spr}} - \Delta W_{\text{dissip}}$, where ΔE_{kin} is the kinetic energy of the top wall, ΔW_{spr} is the work done by the spring force, and ΔW_{dissip} is the friction dissipation contributed from the surface force W_y . Since the variations of friction force (F_y) and surface force (W_y) are available from MD simulation [the inset in Fig. 4(b)], integration of these two force terms with respect to the slip distance gives $\Delta W_{\text{spr}} = 5.13$ nN \cdot Å and $\Delta W_{\text{dissip}} = 4.73$ nN \cdot Å, respectively. The kinetic energy of the top wall at the moment is $\Delta E_{\text{kin}} = 1/2 M v_{\text{slip}}^2 = 0.522$ nN \cdot Å. These quantities clearly show that the original elastic energy stored in the spring during the stick is transferred into the friction dissipation in the solidlike film and subsequent ringing vibrations contributed from the kinetic energy of the top wall. However, the variation of the potential energy term ΔE_p in the solidified film, which cannot be included in the above dynamic equation, is seen in the inset in Fig. 4(a). Simulation shows that the potential energy stored in the solidified film begins to release right after the slip and proceeds over a few nanoseconds. This decay in potential energy by ~ 2.3 nN \cdot Å compensates the one accumulated in the film during the stick.

We conclude that friction dissipation during a stick-slip cycle in boundary lubrication is the one where, during the stick, the total external work done by the driving block is transmitted to the elastic energy stored in the driving spring and the potential energy stored in the solidified film. The former takes about 70% of the total energy. During the slip, more than 90% of the elastic energy in the spring, or 60% of the total energy, is dissipated as friction heating by interlayer slips and wall slips. The remaining 40% of the

total energy is dissipated as the potential energy release in the solidified film and the momentum loss of the top wall during the subsequent mechanical oscillations prior to the instant of new stick. This part of energy dissipation takes a fairly large portion of the total energy for the present molecular system, compared to the estimate from the surface force balance experiment [12].

For the current molecular system, we have also investigated the effect of normal force and the sliding direction on the stick-slip phenomenon. Simulation results showed that all these factors do not change the stick-slip behavior. Furthermore, shear dilation during the slip [13] was not observed. An open question concerns how the elastic shear waves of confining walls affect the critical velocity of stick-slip friction [24,27] and how the elastic deformations of mica and realistic organic model lubricants, such as OMCTS, contribute to the increase of potential during the friction (the present study focuses only on single-atom molecules). These questions will be explored in future studies. We point out that the nanometer length scale of the confined material and nanosecond time scale of the stick-slip event observed in the MD simulation are quite short compared with surface force experiments, which are in a few tens of micrometers length scale and in a few seconds time scale. However, the physics observed in MD simulation and in surface force experiments should be the same. The elegance of the small quantity of the material studied in the MD simulation is its fast relaxation towards equilibrium, allowing the complicated dynamic phenomenon to proceed in a much shorter time.

This work was supported by the U.S. Air Force Office of Scientific Research (FA9550-08-1-0214), the National Science Foundation (NSF 0904287), and the National Energy Research Scientific Computing Center.

*leng@gwu.edu

- [1] F. P. Bowden and D. Tabor, *The Friction and Lubrication of Solids* (Clarendon, Oxford, 1964).
- [2] M. Urbakh *et al.*, *Nature (London)* **430**, 525 (2004).
- [3] J. N. Israelachvili, P. M. McGuiggan, and A. M. Homola, *Science* **240**, 189 (1988).
- [4] J. Klein and E. Kumacheva, *Science* **269**, 816 (1995).
- [5] J. Klein and E. Kumacheva, *J. Chem. Phys.* **108**, 6996 (1998).
- [6] E. Kumacheva and J. Klein, *J. Chem. Phys.* **108**, 7010 (1998).
- [7] M. L. Gee *et al.*, *J. Chem. Phys.* **93**, 1895 (1990).
- [8] H. Yoshizawa and J. Israelachvili, *J. Phys. Chem.* **97**, 11 300 (1993).
- [9] M. Schoen *et al.*, *Science* **245**, 1223 (1989).
- [10] P. A. Thompson and M. O. Robbins, *Science* **250**, 792 (1990).
- [11] P. A. Thompson, M. O. Robbins, and G. S. Grest, *Isr. J. Chem.* **35**, 93 (1995).
- [12] J. Klein, *Phys. Rev. Lett.* **98**, 056101 (2007).
- [13] M. H. Muser, M. Urbakh, and M. O. Robbins, in *Advances in Chemical Physics* (Wiley, New York, 2003), Vol. 126, p. 187.
- [14] O. M. Braun, *Tribol. Lett.* **39**, 283 (2010).
- [15] Y. S. Leng, *J. Phys. Condens. Matter* **20**, 354017 (2008).
- [16] Y. J. Lei and Y. S. Leng, *Phys. Rev. E* **82**, 040501 (2010).
- [17] H. K. Christenson, *J. Chem. Phys.* **78**, 6906 (1983).
- [18] R. G. Horn and J. N. Israelachvili, *J. Chem. Phys.* **75**, 1400 (1981).
- [19] M. P. Allen and D. J. Tildesley, *Computer Simulation of Liquids* (Clarendon, Oxford, 1987).
- [20] H. Matsubara, F. Pichierri, and K. Kurihara, *J. Chem. Phys.* **134**, 044536 (2011).
- [21] G. He, M. H. Muser, and M. O. Robbins, *Science* **284**, 1650 (1999).
- [22] Indeed, in our previous studies [Y. S. Leng and P. T. Cummings, *Phys. Rev. Lett.* **94**, 026101 (2005); *J. Chem. Phys.* **125**, 104701 (2006)], we found that applying a thermostat perpendicular to the shear direction yields no difference of the friction behavior of confined fluids, as long as the sliding velocity is sufficiently small compared with the thermal motion of the particles.
- [23] M. O. Robbins and P. A. Thompson, *Science* **253**, 916 (1991).
- [24] B. Q. Luan and M. O. Robbins, *Phys. Rev. Lett.* **93**, 036105 (2004).
- [25] Based on the shear-melting model, Klein [12] suggested that the surface force can be represented by a viscous damping term $B(dx/dt)$. The relation between this damping term and the effective viscosity η_{eff} was given by $B(dx/dt) = (A\eta_{\text{eff}}/D)(dx/dt)$, where A is the contact area and D is the gap distance. An analytic solution given by Klein was used to fit the shear-melting curve. We find that for the confined argon film $\eta_{\text{eff}} = 0.72$ Pa s, about 3 orders of magnitude larger than the bulk value. Interestingly, for the OMCTS film in the surface force balance experiment, Klein found the effective viscosity during the slip is about 4 orders of magnitude larger than the bulk viscosity of OMCTS.
- [26] B. A. Younglove and H. J. M. Hanley, *J. Phys. Chem. Ref. Data* **15**, 1323 (1986).
- [27] B. N. J. Persson, *Sliding Friction: Physical Principles and Applications* (Springer, New York, 2000).